Carbohydrate Polymers 97 (2013) 384–390

Contents lists available at SciVerse ScienceDirect

Carbohydrate Polymers

journal homepage: www.elsevier.com/locate/carbpol

# $^{1}H$ and $^{13}C$ chemical shift assignment of the monomers that comprise carboxymethyl cellulose

Hiroyuki Kono*

*Department of Science and Engineering for Materials, Tomakomai National College of Technology, Nishikioka 443, Tomakomai, Hokkaido 059-1275, Japan*

ARTICLE INFO

*Article history:*
Received 17 January 2013
Received in revised form 19 April 2013
Accepted 16 May 2013
Available online 23 May 2013

*Keywords:*
Carboxymethyl cellulose
NMR
Chemical shift assignment
Substitution distribution
Conformation

ABSTRACT

$^{1}H$ and $^{13}C$ chemical shift assignment of the anhydroglucose units (AGUs) that comprise sodium carboxymethyl cellulose (CMC) with a degree of substitution (DS) of 0.70 was performed using 2D NMR spectra obtained from COSY, TOCSY, HSQC, and HSQC–TOCSY experiments. In the 2D COSY and TOCSY spectra, there are eight correlation networks for the H1 to H6′ atoms of AGU; each $^{1}H$ resonance of the eight AGUs was assigned from the changes in the intensities of the resonances with mixing times during the TOCSY experiments. The ring $^{13}C$ resonances were assigned via analysis of HSQC–TOCSY spectra and confirmed via the HSQC spectra. Comparison of the shift data enabled the assignment of the eight AGUs as two types of both 2,3,6-tri-O- and 3,6-di-O-carboxymethylated, one type each of 2,6-di-O-, 2-mono-O-, and 6-mono-O-carboxymethylated AGU, and unsubstituted AGU. The obtained shift data will also be useful for characterization of the substitution distribution of other cellulose derivatives.



## 1. Introduction

Carboxymethyl cellulose (CMC) is one of the most important cellulose derivatives, and is used in the fields of food, pharmaceuticals, cosmetics, and paint as a viscosity modifier, thickener, emulsion stabilizer, water-retention agent, etc. CMC is obtained from the reaction of the hydroxyl groups at the 2, 3, and 6 positions of the anhydroglucose units (AGUs) of cellulose with chloroacetic acid; this reaction generally results in nonuniform distribution of carboxymethyl (CM) substituents. Therefore, in the CMC structure, eight different AGU monomers, namely unsubstituted AGU and 2,3,6-tri-O-, 2,3-di-O-, 2,6-di-O-, 3,6-di-O-, 2-mono-O-, 3-mono-O-, and 6-mono-O-carboxymethyl substituted AGU, randomly exist along the chain (Heinze & Liebert, 2001). Although elucidation of the substituent distribution is important to understanding the structure–property relationships of CMC, there is no conventional method for determining the molecular structure owing to its complexity.

To date, a large number of publications have focused on the determination of the substituted distribution in CMC (de la Motte, Hasani, Brelid, & Westman, 2011; Gautier & Lecourtier, 1991; Glinel, Sauvage, Oulyadi, & Huguet, 2000; Gronski & Hellmann, 1997; Heinze, Erler, Nehls, & Klemm, 1994; Ho & Klosiewicz, 1980; Marle, Charpentier, Mocanu, & Chapelle, 1999; Niemela & Sjöstrom, 1988, 1989; Reuben & Conner, 1983; Saake, Horner, Puls, Heinze, & Koch, 2001; Tezuka, Tsuchiya, & Shiomi, 1996; Zeller, Griesgraber, & Gray, 1991). Among these, quantitative NMR (de la Motte et al., 2011; Gautier & Lecourtier, 1991; Glinel et al., 2000; Gronski & Hellmann, 1997; Ho & Klosiewicz, 1980; Marle et al., 1999; Reuben & Conner, 1983; Tezuka et al., 1996; Zeller et al., 1991) and/or HPLC analysis (Heinze et al., 1994; Niemela & Sjöstrom, 1988, 1989; Saake et al., 2001) of oligomers and monomers obtained by acid or enzymatic hydrolysis of CMC are traditionally used. These methods, however, require some pretreatment processes. With respect to direct methods for determining the substitution distribution of CMC without pretreatment, quantitative analysis of the methylene and carbonyl carbon resonances in the $^{13}C$ NMR spectrum of CMC has been reported (Kamide et al., 1985); however, the carbon resonances overlap within a narrow region in the spectrum. In addition, although limited information about the substitution distribution could be obtained from the characteristic C1, C4, and C6 resonances of CMC, it is impossible to obtain detailed information such as the substitution distribution and monomer composition of the structures from these resonances owing to a lack of precise assignments (Kamide et al., 1985; Zeller et al., 1991).

In this study, the assignment of ring carbon and proton resonances in the NMR spectra of CMC was performed via 2D NMR experiments, including COSY (Derome & Williamson, 1990; Rance et al., 1983), TOCSY (Bax & Davis, 1985; Braunschweiler & Ernst, 1983), HSQC–TOCSY (Duus, Gotfredsen, & Bock, 2000; Kover, Hruby, & Uhrin, 1997; Parella, 1998; Willker, Leibfritz, Kerssebaum, & Bermel, 1993), and HSQC (Bax, Griffey, & Hawkins, 1983; Bax & Subramanian, 1986), on CMC (degree of substitution (DS) = 0.70). In the TOCSY spectra of CMC, eight sets of through-bond $^{1}H$–$^{1}H$

* Tel.: +81 144 67 8036; fax: +81 144 67 8036.
*E-mail address:* kono@sem.tomakomai-ct.ac.jp

0144-8617/$ – see front matter © 2013 Elsevier Ltd. All rights reserved.
http://dx.doi.org/10.1016/j.carbpol.2013.05.031

correlation connectivities from H1 to H6′ of AGU, which CMC is composed of, were observed, and all protons in the eight AGUs could be assigned. In addition, the $^{13}C$ resonances of the ring carbons in the eight AGUs were assigned using HSQC–TOCSY and HSQC spectra. On the basis of the chemical shift data obtained from the analyses of these 2D spectra, the substitution patterns of the eight AGUs were determined. In addition, the C6 chemical shift suggests that the C6 substituent conformation depends on the substitution of the C2 of the vicinal AGU; these results are also described herein.

## 2. Experimental

### 2.1. Materials

CMC powder (weight average molecular weight of 250 000, DS = 0.70) was purchased from Acros Organics Co., Ltd. (Belgium) and used as received. Deuterium oxide ($D_2O$; 99.9% isotopic purity) containing 4,4-dimethyl-4-silapentane-1-sulfonic acid (DSS) as an internal standard was purchased from Sigma–Aldrich Co. (USA). NMR tubes (5 mm outer diameter) were purchased from Wilmad-Labglass Co. (USA).

### 2.2. NMR spectroscopy

A 3 mg sample of CMC dissolved in 0.6 mL of $D_2O$ in a 5 mm NMR tube was used for all NMR experiments. All NMR spectra were recorded at 343 K on a Bruker BioSpin AVIII 500 spectrometer (Germany, $^1H$ frequency of 500.13 MHz, $^{13}C$ frequency of 125.13 MHz) equipped with a 2-channel BBO probe incorporating a *z*-gradient coil. Using this spectrometer, the following experiments were performed: 1D $^1H$, 1D $^{13}C$, water-suppressed 2D $^1H$–$^1H$ COSY using gradient pulse for selection (Trimbre & Bernstein, 1994), water-suppressed 2D $^1H$–$^1H$ TOCSY using the MLEV17 sequence (Bax & Davis, 1985; Braunschweiler & Ernst, 1983) for TOCSY spin-locking, 2D $^1H$–$^{13}C$ HSQC via INEPT transfer (Bax et al., 1983; Bax & Subramanian, 1986) using Echo/Antiecho-TPPI gradient selection (Kay, Keifer, & Saarinen, 1992) with $^1H$ decoupling during acquisition using trim pulses (Bax & Davis, 1985; Braunschweiler & Ernst, 1983) in INEPT transfer, and 2D $^1H$–$^{13}C$ HSQC–TOCSY via double INEPT transfer using sensitivity improvement and DIPSI2 (Rucker & Shaka, 1989) for Hartman–Hahn mixing (Bax & Davis, 1985; Braunschweiler & Ernst, 1983). In the COSY experiments, a total of 256 $t_1$ acquisitions with 32 scans per increment were collected. In the TOCSY experiments, the mixing times were 50, 100, or 180 ms, and a total of 256 $t_1$ acquisitions with 64 scans per increment were collected. In the HSQC experiments, the delay time was 3.44 ms, which corresponds with a $J_{C-H}$ of 145 Hz, and a total of 196 $t_1$ acquisitions with 128 scans per increment were collected. In the HSQC–TOCSY experiments, the contact time was 3.75 ms, the Hartman–Hahn mixing times (Bax & Davis, 1985; Braunschweiler & Ernst, 1983) were set at 100 or 180 ms, and a total of 196 $t_1$ acquisitions with 128 scans per increment were collected. The repetition time was 2.0 s for all the NMR experiments. The $^1H$ and $^{13}C$ chemical shifts of the NMR data were calibrated by assigning the methyl peak of DSS as 0 ppm.

## 3. Results

Fig. 1 shows $^1H$ and $^{13}C$ NMR spectra of CMC in $D_2O$ recorded at 343 K. In the $^1H$ spectrum, a plethora of $^1H$ resonances from the AGUs that compose the CMC structure overlap in the narrow region 5.0–3.0 ppm. As each AGU contains seven protons, i.e., H1–H6′, in the glucose ring and additional methylene protons in the substituted carboxymethyl groups, information about the structure of CMC could not be obtained from the $^1H$ NMR spectrum. In the $^{13}C$ NMR spectrum, which is no more complex than the $^1H$ NMR spectrum, the carbonyl carbons of the substituent groups and C1 and C6 of the glucose ring appear at 182–178, 106–104, and 72–61 ppm, respectively, as previously assigned (Kamide et al., 1985), while the resonances for the ring carbons in the 2–5 positions appear as complex spectral lines in the region of 89–73 ppm. Therefore, further $^1H$ and $^{13}C$ chemical shift assignment of the AGUs in CMC is necessary to obtain detailed structural information such as the distribution of substituents at the 2, 3, and 6 positions, and the number of 2,3,6-tri-O-, 2,3-di-O-, 2,6-di-O-, 3,6-di-O-, 2-mono-O-, 3-mono-O-, 6-mono-O-, and un-carboxymethylated AGUs in the molecular structure.

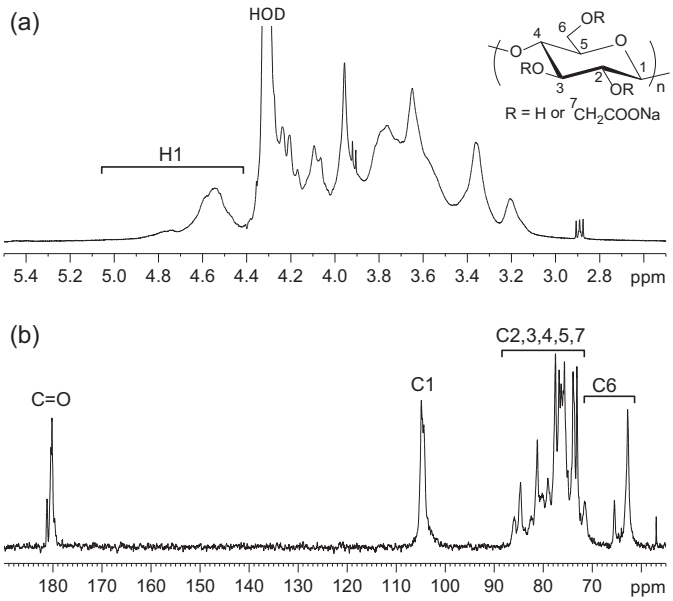


**Fig. 1.** (a) $^1H$ and (b) $^{13}C$ NMR spectra of CMC (DS = 0.70) in $D_2O$ recorded at 343 K.

Fig. 2 shows the contour plot of a COSY spectrum, which identifies direct $^1H$–$^1H$ couplings, with a stacked TOCSY spectrum recorded with a spin-lock time of 50 ms. The TOCSY spectrum reveals through-bond long-range $^1H$–$^1H$ couplings as well as vicinal $^1H$–$^1H$ couplings; longer spin-lock times provide longer range $^1H$–$^1H$ correlations because the polarization expands through more bonds in an isolated spin system such as AGU. Therefore, $^1H$ resonance assignment of each AGU that comprises CMC was possible through a comparison of the specific correlation signals observed in the TOCSY correlation maps recorded with different spin-lock times. Fig. 3 shows the through-bond correlations from H1 with other ring protons in expanded partial COSY and TOCSY spectra recorded with spin-lock times of 50, 100, and 180 ms. In the COSY spectrum, as denoted by dotted lines, at least eight different H1–H2 couplings were detected, although the correlation peaks partially overlapped. Here, the eight types of AGUs with H1 resonances appearing at 4.67, 4.65, 4.60, 4.56, 4.55, 4.53, 4.50, and 4.48 ppm, are referred to as residue A, B, C, D, E, F, G, and H, respectively. In the TOCSY spectra, a 50 ms spin-lock time provides through-bond correlations from H1 to H3 in addition to those from H1 to H2 in AGUs A–H. Similarly, through-bond correlations from H1 to H2–H5 were detected using 100 ms of spin-lock time, and correlations from H1 to all protons in each AGU were detected using 180 ms of spin-lock time. The row slices taken from the contour plots of the COSY and TOCSY spectra at the chemical shifts of the H1 proton in AGUs A–H enabled us to clearly assign all protons in the AGUs; however, the spin multiplets of almost all the protons could not be determined because of partially overlapping signals. The $^1H$ assignment of AGUs A–H is shown in Fig. 4, which shows the row slices of the TOCSY

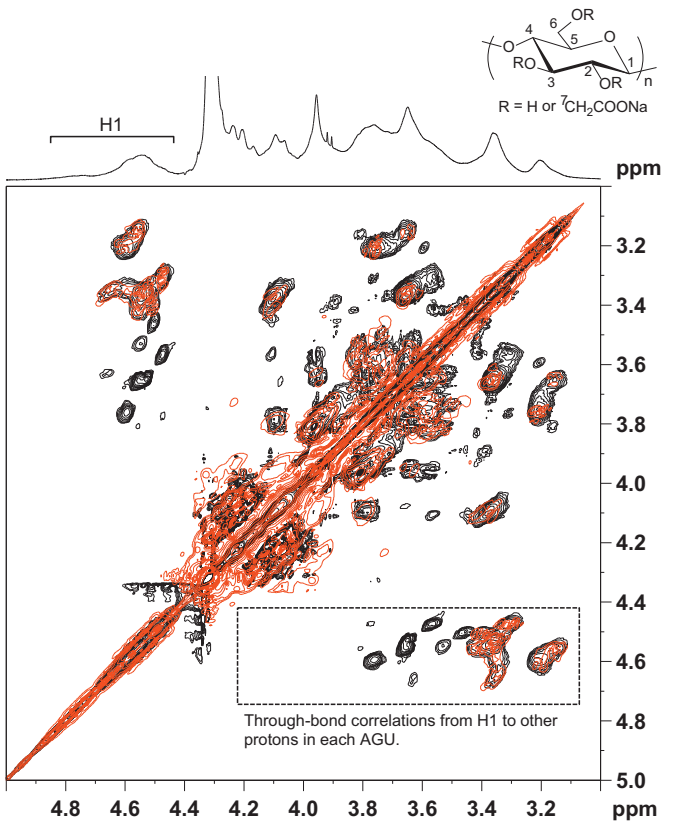


**Fig. 2.** Contour plots of COSY (red lines) and TOCSY (black line) spectra of CMC (DS = 0.70) in $D_2O$ recorded at 343 K. The spin-lock time of the TOCSY experiment was 50 ms. (For interpretation of the references to color in this figure legend, the reader is referred to the web version of this article.)

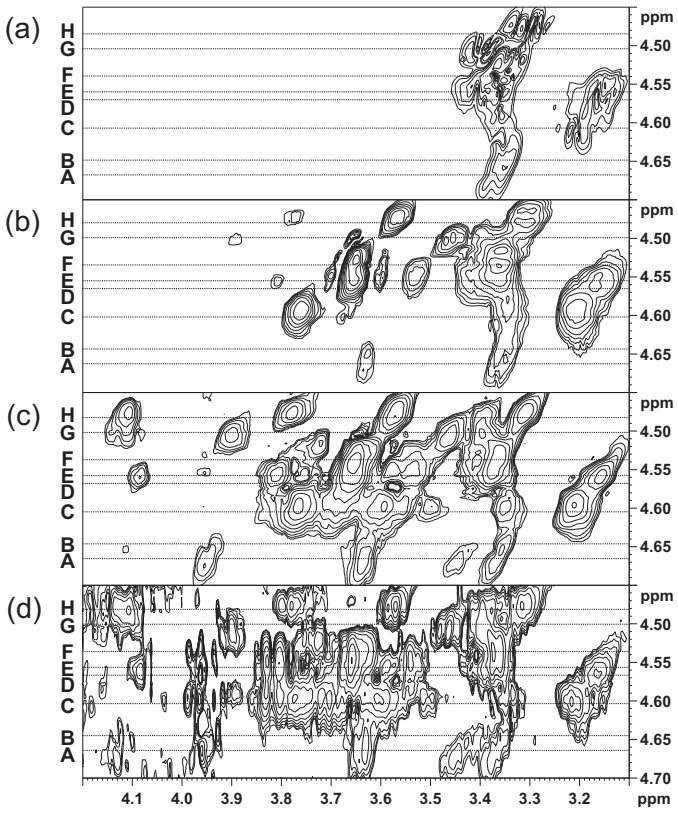


**Fig. 3.** Partial expansion of the contour plots of (a) COSY and (b–d) TOCSY spectra of CMC (DS = 0.70) in $D_2O$ recorded at 343 K. The TOCSY spectra in (b), (c), and (d) were recorded with spin-lock times of 50, 100, and 180 ms, respectively. Correlation peaks observed on the dotted lines indicate through-bond $^1H$–$^1H$ couplings from H1 to the other ring protons in AGUs A–H.

spectrum recorded using 180 ms of spin-lock time; the $^1H$ chemical shifts are summarized in Table 1.

Next, the $^{13}C$ chemical shifts of the ring carbons in each AGU were assigned via analysis of the HSQC and HSQC–TOCSY spectra shown in Fig. 5. Since the directly coupled $^{13}C$ and $^1H$ correlations of over eight AGUs overlap in this region, it was difficult to assign the $^{13}C$ chemical shifts of AGUs A–H using only the HSQC spectrum. Thus, before analyzing the correlation peaks observed via HSQC, the positions of the carbon peaks for each AGU were estimated from the HSQC–TOCSY spectrum recorded with a TOCSY spin-lock time of 180 ms that is shown in Fig. 6. In this spectrum, through-bond correlations from H1 to all ring carbons in AGU (C2–C6) were evident; using these data, the $^{13}C$ chemical shifts of the ring carbons of each AGU in the complex 1D $^{13}C$ NMR spectrum were assigned. For example, the H1 resonance of AGU C at 4.59 ppm correlates with $^{13}C$ resonances at 84.8, 80.0, 76.0 and 63.0 ppm, which indicates that these resonances correspond to C2, C3, C4, C5, and C6 of AGU C and that two of the carbon signals overlap. Similarly, the $^{13}C$ chemical shifts of AGUs A–H were assigned, as shown in the 1D $^{13}C$ spectrum displayed left of the 2D contour plot of the HSQC–TOCSY spectrum. On the basis of the results obtained from the HSQC–TOCSY spectrum and the $^1H$ chemical shift data summarized in Table 1, correlations of directly bonded $^1H$–$^{13}C$ moieties in AGUs A–H observed in the HSQC spectrum were easily assigned, as indicated in Fig. 7. The $^{13}C$ chemical shift data for AGUs A–H are also summarized in Table 2.

## 4. Discussion

In this study, CMC (DS = 0.70) was analyzed via 2D NMR measurements using a 500 MHz instrument; accordingly, at least eight AGUs (denoted A–H) are observed in the 2D correlation maps. These

**Table 1**
$^1H$ chemical shift assignment (ppm) of AGUs A–H from CMC (DS = 0.70) dissolved in $D_2O$ at 343 K.

| AGU | H1 | H2 | H3 | H4 | H5 | H6 | H6′ | Monomer unit |
|---|---|---|---|---|---|---|---|---|
| A | 4.67 | **3.37** | **3.65** | 3.94 | 3.66 | **4.10** | **3.38** | 2,3,6-Tri-O-CM-Glc |
| B | 4.64 | **3.36** | **3.63** | 3.91 | 3.66 | **4.10** | **3.38** | 2,3,6-Tri-O-CM-Glc |
| C | 4.61 | **3.21** | 3.76 | 3.72 | 3.58 | 3.96 | 3.80 | 2-Mono-O-CM-Glc |
| D | 4.57 | **3.16** | 3.66 | 3.80 | 3.74 | **4.10** | **3.38** | 2,6-Di-O-CM-Glc |
| E | 4.55 | 3.37 | **3.54** | 3.80 | 3.60 | **4.10** | **3.38** | 3,6-Di-O-CM-Glc |
| F | 4.54 | 3.37 | 3.66 | 3.66 | 3.58 | 3.96 | 3.80 | Unsubstituted glucose |
| G | 4.50 | 3.42 | **3.46** | 3.90 | 3.57 | **4.10** | **3.38** | 3,6-Di-O-CM-Glc |
| H | 4.43 | 3.32 | 3.57 | 3.80 | 3.57 | **4.10** | **3.38** | 6-Mono-O-CM-Glc |

CM, carboxymethyl, Glc, glucose.
Chemical shifts of the substituted positions are indicated by boldface in this table.

**Table 2**
$^{13}C$ chemical shift assignment (ppm) of AGUs A–H in CMC (DS = 0.70) dissolved in $D_2O$ at 343 K.

| AGU | C1 | C2 | C3 | C4 | C5 | C6 | Monomer unit |
|---|---|---|---|---|---|---|---|
| A | 104.7 | **82.3** | **82.3** | 82.4 | 75.5 | **65.5** | 2,3,6-Tri-O-CM-Glc |
| B | 104.7 | **82.6** | **82.5** | 82.5 | 75.5 | **65.5** | 2,3,6-Tri-O-CM-Glc |
| C | 104.7 | **84.7** | 76.0 | 80.2 | 77.6 | 62.7 | 2-Mono-O-CM-Glc |
| D | 104.5 | **84.7** | 75.5 | 79.1 | 76.0 | **65.5** | 2,6-Di-O-CM-Glc |
| E | 104.5 | 75.7 | **86.1** | 79.1 | 76.9 | **65.5** | 3,6-Di-O-CM-Glc |
| F | 104.9 | 75.7 | 76.8 | 81.2 | 77.6 | 62.7 | Unsubstituted glucose |
| G | 105 | 74.3 | **85.7** | 78.4 | 76.5 | **65.5** | 3,6-Di-O-CM-Glc |
| H | 105 | 75.4 | 76.5 | 79.1 | 76.5 | **65.5** | 6-Mono-O-CM-Glc |

CM, carboxymethyl, Glc, glucose.
Chemical shifts of the substituted positions are indicated by boldface in this table.

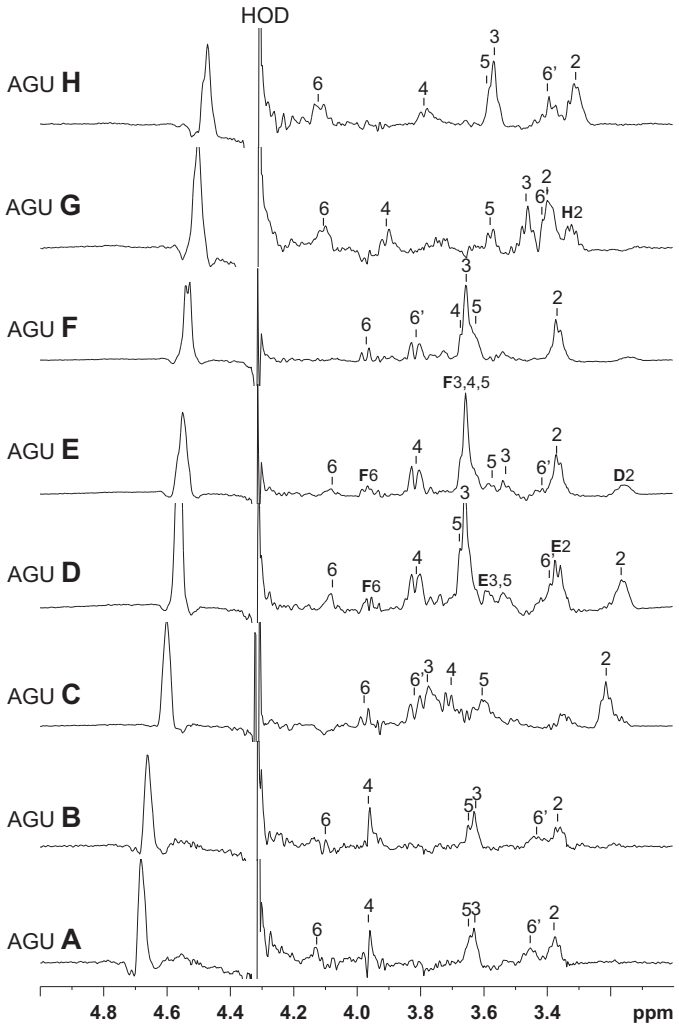


**Fig. 4.** Series of 1D spectra from row slices along the horizontal axis of the TOCSY spectrum recorded with a spin-lock time of 180 ms displayed in Fig. 3(d). These slices were taken at the diagonal peaks of the H1 resonances of AGUs A–H appearing at 4.67, 4.64, 4.61, 4.57, 4.55, 4.54, 4.50, and 4.43 ppm, respectively. The proton assignments are indicated at the signals.

AGUs could be either unsubstituted, 2-mono-, 3-mono-, 6-mono-, 2,3-di-, 2,6-di-, 3,6-di-, or 2,3,6-tri-O-carboxymethyl glucose units. With respect to the monomer composition of CMC, Saake et al. quantified the mole fractions of these monomer components in CMC samples with different DS values using HPLC following acid hydrolysis of the samples and reported that the major monomer in CMC is uncarboxymethylated glucose up to a DS of 0.8 (Saake et al., 2001). In all 2D spectra presented in this study, the intensities of the correlation peaks of AGU F were significantly higher than those of the other correlations, which indicates that residue F is unsubstituted AGU; this assignment is also supported by the C4 chemical shift of AGU F, which appears at 81.2 ppm; this C4 chemical shift has been identified as belonging to the unsubstituted AGU of CMC. Using the $^{1}H$ and $^{13}C$ chemical shifts of AGU F as a reference, the substitution pattern of the other seven AGUs could be determined. Generally, etherification occurs at positions 2, 3, and 6; this exerts a β-effect (Bubb, 2003) on the chemical shift of the substituted carbon atom resulting in a significant downfield shift of 4–10 ppm (Adeyeye, Jansson, Kanne, & Widmalm, 1991; Bubb, 2003; Capitani, Porro, & Segre, 2000). As summarized in Table 1, the C2 chemical shifts of AGUs A, B, C, and D, which appear at 82.3, 82.6, 84.7, and 84.7 ppm, respectively, are shifted ~7–9 ppm downfield from the C2 chemical shift of AGU F (75.7 ppm), while those

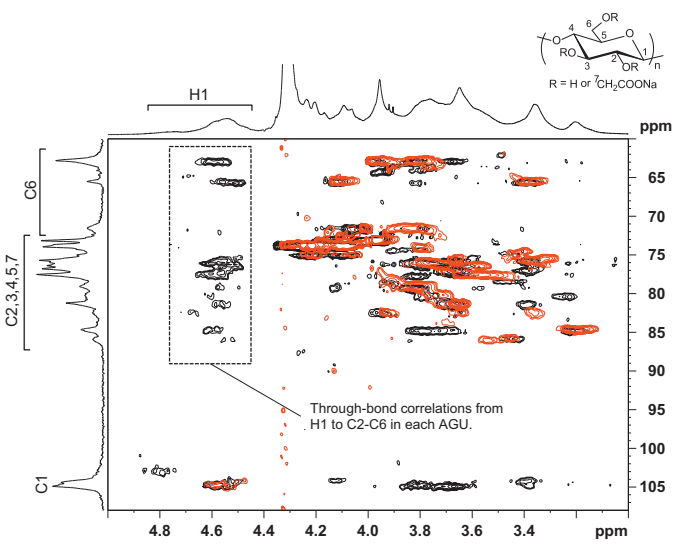


**Fig. 5.** Contour plots of HSQC (red lines) and HSQC-TOCSY (black lines) spectra of CMC (DS = 0.70) in $D_2O$ recorded at 343 K. The contact time of the HSQC and HSQC–TOCSY experiments was 3.75 ms to optimize the $J_{C-H}$ (145 Hz). The spin-lock time in the HSQC-TOCSY experiment was 180 ms. (For interpretation of the references to color in this figure legend, the reader is referred to the web version of this article.)

of AGUs E, G, and H (75.7, 74.3, and 75.4 ppm, respectively) are almost equivalent to the C2 chemical shift of AGU F. This indicates that carboxymethylation occurred at C2 of AGUs A–D. Similarly, the C3 chemical shifts of AGUs A, B, E, and G at 82.3, 82.5, 86.1, and 85.7 ppm, respectively, are shifted 4–10 ppm from the C3 chemical shift of AGU F at 76.8 ppm, while the C3 resonance shifts of AGUs

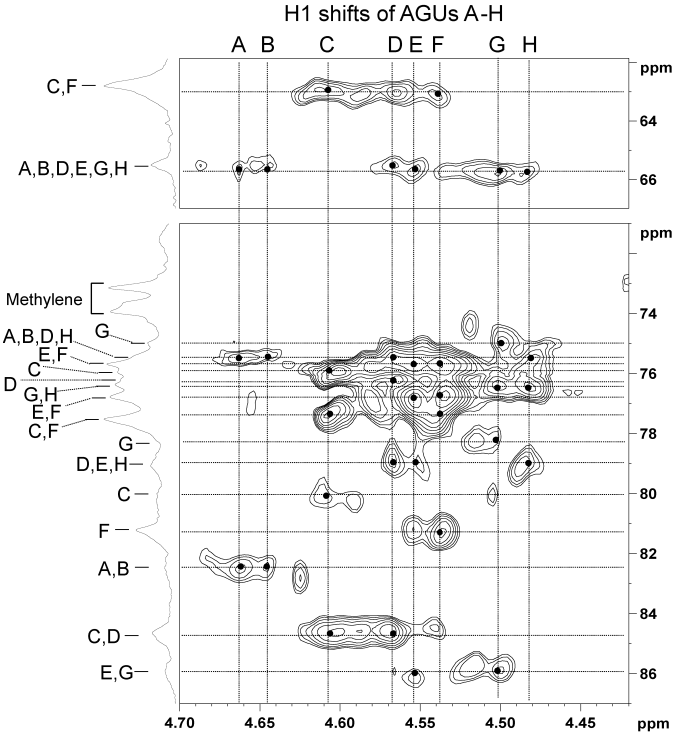


**Fig. 6.** Partial expansion of a contour plot of the HSQC–TOCSY spectrum displayed in Fig. 5. Correlation peaks in the spectrum indicate through-bond $^{1}H$–$^{13}C$ correlations from H1 to the carbon atoms in AGUs A–H. The $^{13}C$ chemical shift of each AGU was assigned from the correlation peaks appearing at the $^{1}H$ signals of each H1 of AGUs A–H. The $^{13}C$ assignments are indicated in the 1D $^{13}C$ spectrum shown along the left axis of the contour plot.

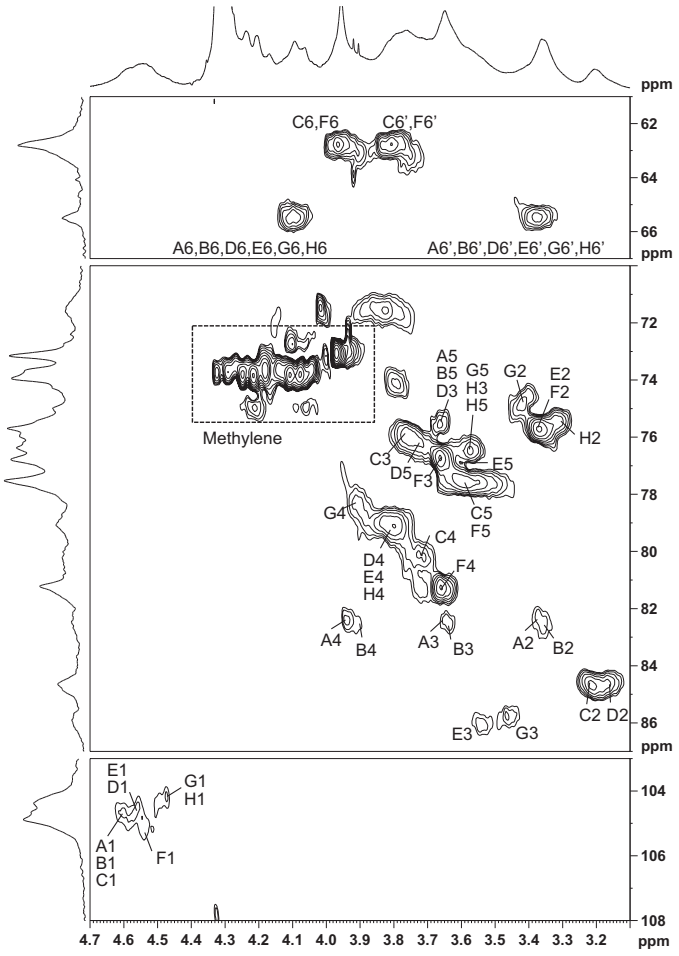


**Fig. 7.** Partial expansion of the contour plot of HSQC spectrum displayed in Fig. 5. The resulting assignments of the correlation peaks are indicated in this figure.

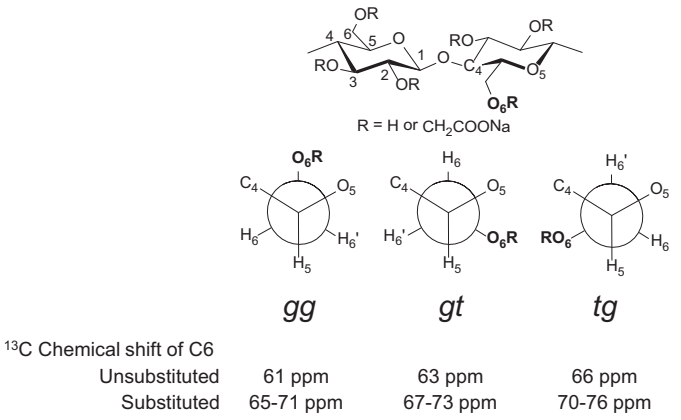


| $^{13}$C Chemical shift of C6 | gg | gt | tg |
|---|---|---|---|
| Unsubstituted | 61 ppm | 63 ppm | 66 ppm |
| Substituted | 65-71 ppm | 67-73 ppm | 70-76 ppm |

**Fig. 8.** CMC gg, gt, and tg conformations around the O6–C6–C5–O5 torsion angle, and $^{13}$C chemical shifts of unsubstituted C6 in each conformation, as proposed by Horii et al. (1983). Substituted C6 chemical shifts in each conformation could be determined by accounting for the β-effect of the C6 substituent.

C (76.0 ppm), D (75.5 ppm), and H (76.5 ppm) are similar to that of AGU F; this indicates that C3 is substituted in AGUs A, B, E, and G. Among the C3-substituted AGUs, the C3 chemical shifts of AGU A and B, which appear at 82.3–82.5 ppm, are slightly shifted from those of AGU E and G, which appear at 85.7–86.1 ppm; this difference is considered to be due primarily to the presence or absence of vicinal substituents at C2: the C2s of AGUs E and G are bonded to free hydroxyl groups, while AGUs A and B are substituted at both C2 and C3. Accordingly, the C3s of AGUs A and B experience the γ-effect (Bubb, 2003) from the C2 substituents. The γ-effect is considered to be minor in comparison to the β-effect and is of the order of 1 to 3 ppm (Adeyeye et al., 1991; Bubb, 2003; Capitani et al., 2000). The γ-effect from the C3 substituents was also confirmed by the C2 chemical shifts of the 2-O-carboxymethylated AGUs (i.e., A, B, C, and D): The C2 chemical shifts of AGUs A and B are 82.3 and 82.6 ppm, respectively, while those of AGUs C and D are 84.7 ppm. This indicates that the C2s of AGUs A and B, which are substituted at the C3 position, experience the γ-effect from the C3 substituents resulting in a ~2 ppm upfield shift.

The C6 chemical shifts of AGUs C and F are equivalent and appear at 62.7 ppm; the C6 chemical shifts of the other AGUs (65.5 ppm) were shifted downfield by 2.8 ppm indicating that the C6s of AGUs A, B, D, E, G, and H are substituted. However, as described above, the β-effect caused by substitution would normally cause a 4–10 ppm downfield shift; therefore, the C6 downfield shift observed in six of the AGUs could not be explained only by the β-effect of C6 substitution. Thus, it is considered that a conformation change via rotation around the O6–C6–C5–O5 torsion angle accompanies substitution at C6. With respect to this torsion angle in mono-, oligo-, and polysaccharides including cellulose (Fig. 8), Horii, Hirai, and Kitamaru (1983) suggested that gauche–gauche (gg), gauche–trans (gt), and trans–gauche (tg) conformations lead to C6 chemical shift groupings of 61, 63, and 66 ppm, respectively. In addition, they concluded that crystalline native cellulose takes the tg conformation, while amorphous cellulose and crystalline cellulose II prefer the gt conformation, which indicates that gt is the most stable conformation. In the case of CMC dissolved in solvent, unsubstituted C6 is considered to take a gt conformation because the C6 chemical shifts of AGUs C and F, which are unsubstituted, are both 62.7 ppm. When substitution occurs at position 6 of cellulose, the C6 chemical shifts of gg, gt, and tg conformations are expected to be 65–71, 67–73, and 70–76 ppm, respectively, owing to the β-effect of the substitution (Fig. 8). Therefore, AGUs A, B, D, E, G, and H are considered to take the gg conformation because their C6 chemical shifts are all 65.5 ppm. Although the correlation between chemical shift and conformation proposed by Horii et al. (1983) may not be directly applicable to cellulose derivatives, the preference for the gg conformation has been confirmed in many glucose derivatives. Thus, it is expected that the conformational change from gt to gg occurs with C6 substitution of cellulose.

According to many manuscripts regarding the structure of CMC (de la Motte et al., 2011; Gautier & Lecourtier, 1991; Glinel et al., 2000; Gronski & Hellmann, 1997; Heinze, Heinze, & Klemm, 1999; Ho & Klosiewicz, 1980; Marle et al., 1999; Reuben & Conner, 1983; Tezuka et al., 1996; Zeller et al., 1991), the $^{13}$C resonance at 71.6 ppm in the $^{13}$C spectrum is known to correspond to the substituted C6 signal. In this study, this carbon signal is observed and correlates with two proton resonances at 4.0 and 3.9 ppm in the HSQC spectrum (Fig. 7). The peak at 4.0 ppm is intense, while the peak at 3.9 ppm is relatively weak and broad for a $^{1}$H resonance. Regardless, even the sharp signal at 4.0 ppm could not be observed in the TOCSY spectra (Fig. 3). In addition, in the HSQC–TOCSY spectra, the long-range correlations from the signal at 71.6 ppm are ambiguous in comparison with those from the substituted C6 resonance at 65.5 ppm (Figs. 5 and 6). With respect to the substituted C6 resonances at 71.6 and 65.5 ppm, $^{13}$C NMR spectra of CMC with DS values ranging from 0.99 to 2.95 were previously reported by Kulicke, Kull, Thielking, Engelhardt, and Pannek, 1986). In these spectra, the intensity of the resonance at 71.6 ppm increased with increasing DS, while an inverse relationship was evident for the signal at 65.5 ppm. In addition, the resonance at 65.5 ppm disappeared when the DS of CMC reached 2.29. Therefore, it could be considered that the chemical shift of the substituted C6 shifts from 65.5 to

71.6 ppm with increasing DS: the chemical shift at 65.5 ppm is dominant with low DS, while the chemical shift at 71.6 ppm is dominant with high DS. Considering the β-effect of C6 substitution and the relationship between the $^{13}C$ chemical shift and the O6–C6–C5–O5 torsion angle proposed by Horii et al. (1983), the 65.5 ppm chemical shift corresponds with the gg conformation and the 71.6 ppm chemical shift corresponds with either the gt or tg conformation. The change of the substituted C6 resonance is suggested to be related to the presence or absence of a C2 substituent on the vicinal AGU on the nonreducing side because the steric bulk of the carboxymethyl groups at C6 in a gg conformation would interfere with the C2 substituent of the vicinal AGU (Fig. 8). Therefore, when the hydroxyl group at C2 of the vicinal AGU in the nonreducing side is not substituted, the substituted C6 takes the most stable conformation, i.e., gg, which results in the 65.5 ppm chemical shift. In contrast, when the C2 hydroxyl is substituted, a conformation change from gg to gt or tg is expected in order to avoid steric interactions between the substituents and the resonance of C6 shifts to 71.6 ppm. In this experiment, because a CMC sample with a DS of 0.70 was analyzed and the signal at 71.6 ppm is broad and weak, the conformational difference between the C6s at 65.5 and 71.6 ppm could not be elucidated. However, the $^{13}C$ chemical shift differences between the two resonances are large enough to indicate a conformational difference around the O6–C6–C5–O5 torsion angle (Kono, 2004; Kono, Erata, & Takai, 2002; Kono, Erata, & Takai, 2003; Kono, Numata, Erata, & Takai, 2004). In order to confirm the conformational change around C6 position of AGUs in CMC from gg to tg or gt, $^{13}C$ NMR measurements of two kinds of CMC samples (DS = 0.90 and 1.12, data not shown) were performed. However, more effective and useful data for structure of CMC, for example, new assignment data, conformation, and distribution, could not be obtained from the analysis of these spectra. Thus, similar analysis of the NMR spectrum of highly substituted sample, for example DS > 1.5 will give a solid support of the conformational change around C6 position of CMC proposed herein.

For the elucidation of the conformational change in C6 position of CMC, NMR measurements for the methylcellulose and cellulose acetate with a DS of 0.6–0.7 were performed (data not shown). As a result, the $^{13}C$ chemical shift change derived from the C6 conformational change could not be observed in the spectra of the methyl cellulose and cellulose acetate. From these observations, it is considered that the C6 conformational change of cellulose derivatives depends on the molecular size of the substituent groups. In the case of CMC, CM groups are relatively large, so the substituent groups at C6 interfere with the substituent at C2 of vicinal AGU in the nonreducing side. On the other hand, the methyl or acetyl groups at C6 which are relatively small substituent groups could not have an influence on the substituent at C2 of vicinal AGU. However, more NMR experimental data for various cellulose derivatives are required to reveal the hypothesis of the C6 conformational change.

From the discussion above, AGUs A and B can be assigned as 2,3,6-tri-O-carboxymethyl-, AGU C as 2-mono-O-carboxymethyl-, AGU D as 2,6-di-O-carboxymethyl-, AGUs E and G as 3,6-di-O-carboxymethyl-, and AGU H as 6-mono-O-carboxymethyl-substituted AGU. The different NMR signals of the two AGUs with the same substitution pattern, e.g., AGUs A and B, are results of conformational differences caused by the adjacent monomer units, which result in minute changes in the chemical shifts. In addition, 3-mono-O-carboxymethyl- and 2,3-di-O-carboxymethyl-substituted AGUs were assigned from the 2D COSY and TOCSY spectra; however, there were ambiguous and/or overlapping $^{1}H$–$^{1}H$ correlation peaks except for the correlations of AGUs A–H in the TOCSY spectra, and long-range $^{1}H$–$^{13}C$ correlations were observed at $^{1}H$ chemical shifts of 4.59 and 4.52 ppm in the HSQC–TOCSY spectrum (Fig. 6). Such signals may be attributed to 3-mono-O-carboxymethyl- and 2,3-di-O-carboxymethyl-substituted AGUs. Further NMR measurements using an NMR instrument with a higher magnetic field and high-sensitivity NMR probes would enable full assignment of ambiguous and overlapping signals, which will make it possible to precisely estimate the amounts of the eight different AGU monomers comprising CMC, unsubstituted AGU and 2,3,6-tri-O-, 2,3-di-O-, 2,6-di-O-, 3,6-di-O-, 2-mono-O-, 3-mono-O-, and 6-mono-O-carboxymethyl substituted AGU, as well as the substituent distribution at C2, C3, and C6 of CMC.

## 5. Conclusions

In this study, although I had tried full assignment of all monomers comprising CMC, many $^{1}H$ resonances overlapped each other in all regions of spectra. $^{1}H$ and $^{13}C$ chemical shift of mere 8 AGUs could be assigned in this study, and it is remained that many resonances for other AGUs should be assigned. Therefore, quantitative discussion for the 8 AGUs assigned herein is theoretically impossible because full or most of the resonances for CMC has not been assigned precisely. However, this work is a first research to determine the chemical shift assignment of CMC without degradation of the cellulose chain. In this sense, this research is considered to provide the new information about structure of the randomly substituted cellulose derivatives. Similar 2D NMR measurements of the CMC samples with various DS values in a higher magnetic field NMR instrument would enable full assignment of the monomers. In addition, application of these NMR methods used in this study to other complicated cellulose derivatives will provide new insight into their structures.

## Acknowledgments

This work was supported in part by Grants-in-Aid for Scientific Research C-25410134 from the Japan Society for Promotion of Science (JSPS), and Grants-in-Aids for Adaptable and the seamless technology transfer program through target drive R&D (241FT0160 and AS242Z03384M) from Japan Science and Technology Agency (JST).

## Appendix A. Supplementary data

Supplementary data associated with this article can be found, in the online version, at http://dx.doi.org/10.1016/j.carbpol.2013.05.031.

## References

Adeyeye, A., Jansson, P. E., Kanne, L., & Widmalm, G. (1991). Synthesis and NMR and conformational studies of the four anomeric methyl glycosides of the trisaccharide D-Glcp-(1→2)-D-Glcp-(1→3)-α-D-Glcp. *Journal of the Chemical Society, Perkin Transactions*, *2*(7), 963–973.

Bax, A., & Davis, D. G. (1985). MLEV-17-based two-dimensional homonuclear magnetization transfer spectroscopy. *Journal of Magnetic Resonance*, *65*(2), 355–360.

Bax, A., Griffey, R. H., & Hawkins, B. L. (1983). Correlation of proton and nitrogen-15 chemical shifts by multiple quantum NMR. *Journal of Magnetic Resonance*, *55*(2), 301–315.

Bax, A., & Subramanian, S. (1986). Sensitivity-enhanced two-dimensional heteronuclear shift correlation NMR spectroscopy. *Journal of Magnetic Resonance*, *67*(3), 565–569.

Braunschweiler, L., & Ernst, R. R. (1983). Coherence transfer by isotropic mixing: Application to proton correlation spectroscopy. *Journal of Magnetic Resonance*, *53*(3), 521–528.

Bubb, W. A. (2003). NMR spectroscopy in the study of carbohydrates: Characterizing the structural complexity. *Concepts in Magnetic Resonance Part A*, *19A*(1), 1–19.

Capitani, D., Porro, F., & Segre, A. L. (2000). High field NMR analysis of the degree of substitution in carboxymethyl cellulose sodium salt. *Carbohydrate Polymers*, *42*(3), 283–286.

de la Motte, H., Hasani, M., Brelid, H., & Westman, G. (2011). Molecular characterization of hydrolyzed cationized nanocrystalline cellulose, cotton cellulose and softwood kraft pulp using high resolution 1D and 2D NMR. *Carbohydrate Polymers*, *85*(4), 738–746.

Derome, A., & Williamson, M. J. (1990). Rapid-pulsing artifacts in double-quantum-filtered COSY. *Journal of Magnetic Resonance*, *88*(1), 177–185.

Duus, J. O., Gotfredsen, C. H., & Bock, K. (2000). Carbohydrate structural determination by NMR spectroscopy: Modern methods and limitations. *Chemical Reviews*, *100*(12), 4589–4614.

Gautier, S., & Lecourtier, J. (1991). Structural characterization by $^{13}C$ nuclear magnetic resonance of hydrolysed carboxymethylcellulose. *Polymer Bulletin*, *26*(4), 457–464.

Glinel, G., Sauvage, J. P., Oulyadi, H., & Huguet, J. (2000). Determination of substituents distribution in carboxymethylpullulans by NMR spectroscopy. *Carbohydrate Research*, *328*(3), 343–354.

Gronski, W., & Hellmann, G. (1997). NMR-spektroskopische charakterisierung von carboxymethylcellulose. *Papier*, *41*(12), 668–672.

Heinze, T., Erler, U., Nehls, I., & Klemm, D. (1994). Determination of the substituent pattern of heterogeneously and homogeneously synthesized carboxymethyl cellulose by using high-performance liquid chromatography. *Die Angewandte Makromolekulare Chemie*, *215*(1), 93–106.

Heinze, U., Heinze, T., & Klemm, D. (1999). Synthesis and structure characterization of 2,3-O-carboxymethylcellulose. *Macromolecular Chemistry and Physics*, *200*(4), 896–902.

Heinze, T., & Liebert, T. (2001). Unconventional methods in cellulose functionalization. *Progress in Polymer Science*, *26*(9), 1689–1762.

Ho, F. F. L., & Klosiewicz, D. W. (1980). Proton nuclear magnetic resonance spectrometry for determination of substituents and their distribution in carboxymethylcellulose. *Analytical Chemistry*, *52*(6), 913–916.

Horii, F., Hirai, A., & Kitamaru, R. (1983). Solid-state $^{13}C$-NMR study of conformations of oligosaccharides and cellulose. *Polymer Bulletin*, *10*(7–8), 357–361.

Kamide, K., Okajima, K., Kowsaka, K., Matsui, T., Nomura, S., & Hikichi, K. (1985). Effect of the distribution of substitution of the sodium salt of carboxymethylcellulose on its absorbency toward aqueous liquid. *Polymer Journal*, *17*(8), 909–918.

Kay, L. E., Keifer, P., & Saarinen, T. (1992). Pure absorption gradient enhanced heteronuclear single quantum correlation spectroscopy with improved sensitivity. *Journal of the American Chemical Society*, *114*(26), 10663–10665.

Kono, H. (2004). Two-dimensional magic angle spinning NMR investigation of naturally occurring chitins: Precise $^{1}H$ and $^{13}C$ resonance assignment of α- and β-chitin. *Biopolymers*, *75*(3), 255–263.

Kono, H., Erata, T., & Takai, M. (2002). CP/MAS $^{13}C$ NMR study of cellulose and cellulose derivatives. 2. Complete assignment of the $^{13}C$ resonance for the ring carbons of cellulose triacetate polymorphs. *Journal of the American Chemical Society*, *124*(25), 7512–7518.

Kono, H., Erata, T., & Takai, M. (2003). Determination of the through-bond carbon–carbon and carbon–proton connectivities of the native celluloses in the solid state. *Macromolecules*, *36*(14), 5132–5138.

Kono, H., Numata, Y., Erata, T., & Takai, M. (2004). $^{13}C$ and $^{1}H$ resonance assignment of mercerized cellulose II by two-dimensional MAS NMR spectroscopies. *Macromolecules*, *37*(14), 5310–5316.

Kover, K. E., Hruby, V. J., & Uhrin, D. (1997). Sensitivity- and gradient-enhanced heteronuclear coupled/decoupled HSQC–TOCSY experiments for measuring long-range heteronuclear coupling constants. *Journal of Magnetic Resonance*, *129*(2), 125–129.

Kulicke, W. M., Kull, A. H., Thielking, H., Engelhardt, J., & Pannek, J. B. (1986). Characterization of aqueous carboxymethylcellulose solutions in terms of their molecular structure and its influence on rheological behavior. *Polymer*, *37*(13), 2723–2731.

Marle, L., Charpentier, D., Mocanu, G., & Chapelle, S. (1999). Comparison of the distribution pattern of associative carboxymethylcellulose derivatives. *European Polymer Journal*, *35*(1), 1–7.

Niemela, K., & Sjöstrom, E. (1988). Identification of the products of hydrolysis of carboxymethylcellulose. *Carbohydrate Research*, *180*(1), 43–52.

Niemela, K., & Sjöstrom, E. (1989). Characterization of hardwood-derived carboxymethylcellulose by gas–liquid chromatography and mass spectrometry. *Polymer Communications*, *30*(8), 254–256.

Parella, T. (1998). Pulsed field gradients: A new tool for routine NMR. *Magnetic Resonance in Chemistry*, *36*(7), 467–495.

Rance, M., Sørensen, O. W., Bodenhausen, G., Wagner, G., Ernst, R. R., & Wuthrich, K. (1983). Improved spectral resolution in COSY $^{1}H$ NMR spectra of proteins via double quantum filtering. *Biochemical and Biophysical Research Communications*, *117*(2), 479–485.

Reuben, J., & Conner, H. T. (1983). Analysis of the carbon-13 N.M.R. spectrum of hydrolyzed O-(carboxymethyl)cellulose: Monomer composition and substitution patterns. *Carbohydrate Research*, *115*(16), 1–13.

Rucker, S. P., & Shaka, A. J. (1989). Broadband homonuclear cross polarization in 2D N.M.R. using DIPSI-2. *Molecular Physics*, *68*(2), 509–517.

Saake, B., Horner, S., Puls, J., Heinze, T., & Koch, W. (2001). A new approach in the analysis of the substituent distribution of carboxymethyl celluloses. *Cellulose*, *8*(1), 59–67.

Tezuka, Y., Tsuchiya, Y., & Shiomi, T. (1996). $^{13}C$ NMR determination of substituent distribution in carboxymethylcellulose by use of its peresterified derivatives. *Carbohydrate Research*, *291*(23), 99–108.

Trimbre, L. A., & Bernstein, M. A. (1994). Application of gradients for water suppression in 2D multiple-quantum-filtered COSY spectra of peptides. *Journal of Magnetic Resonance Series B*, *105*(1), 67–72.

Willker, W., Leibfritz, D., Kerssebaum, R., & Bermel, W. (1993). Gradient selection in inverse heteronuclear correlation spectroscopy. *Magnetic Resonance in Chemistry*, *31*(3), 287–292.

Zeller, S. G., Griesgraber, G. W., & Gray, G. R. (1991). Analysis of positions of substitution of O-carboxymethyl groups in partially O-carboxymethylated cellulose by the reductive-cleavage method. *Carbohydrate Research*, *211*(1), 41–45.